Materials Research Express

RECEIVED
22 February 2019

REVISED
5 October 2019

ACCEPTED FOR PUBLICATION
10 October 2019

PUBLISHED
18 October 2019

PAPER

Growth behavior of β-Ga_2O_3 nanowires synthesized by chemical vapor deposition

Lei Shang[1,4], **Yiqian Wang**[2,4], **Meiling Zhuang**[1], **Bing Liu**[2] and **Feng Shi**[3]

[1] Textile & Clothing institute, Qingdao University, No. 308 Ningxia Road, Qingdao, 266071, People's Republic of China
[2] The Cultivation Base for State Key Laboratory, Qingdao University, No. 308 Ningxia Road, Qingdao 266071, People's Republic of China
[3] College of Physics and Electronics, Shandong Normal University, Jinan 250014, People's Republic of China
[4] Authors to whom any correspondence should be addressed.

E-mail: shanglei_79@163.com, yqwang@qdu.edu.cn, zmlqdu@126.com, bing_liu@qdu.edu.cn and sf751106@sina.com.cn

Keywords: β-Ga_2O_3 nanowires, microstructure, CVD, growth mechanism

Abstract

Gallium oxide (Ga_2O_3) nanowires deposited on Si substrates were synthesized by chemical vapor deposition (CVD) of Ga powders with assisted catalyzed by nickel chloride ($NiCl_2$). The microstructure of these nanowires was investigated using high-resolution transmission electron microscopy (HRTEM) and electron energy loss spectroscopy (EELS). Four major types of morphology were observed for these Ga_2O_3 nanomaterials, namely, the particle-fused nanowires, single-crystal nanowires, nanorods and core–shell nanowires. Single crystal and core–shell nanowires were mainly studied. EELS indicated that the amorphous shell was Ga_2O_3. Because metal catalysts were introduced in the growth process, a vapor-solid (VS) growth mechanism was proposed to explain the single crystal Ga_2O_3 nanowires.

1. Introduction

In recent years, the preparation of one-dimensional (1D) single-crystalline conducting oxide nanomaterials has drawn much attention due to their size, morphology-related properties, and their emerging applications in functional nanodevices [1–7]. Monoclinic gallium oxide (β-Ga_2O_3) as a wide-band gap, transparent, conducting oxide (TCO) ($E_g = 4.9$ eV), has great potential applications in optoelectronic nanodevices and gas sensors [8–13]. Although various methods have been used to prepare β-Ga_2O_3 nanomaterials such as physical evaporation [14–16], thermal chemical vapor deposition (CVD) [17, 18], arc-discharge [19], pulse laser deposition (PLD) [20], microwave plasma [21], and carbon thermal reduction [22–25], but so far, the most widely used method is CVD, which has the advantages of flexibility, simple equipment, convenient operation and maintenance, high production efficiency, high output and low pressure required for processing. However, there are few papers on the synthesis of gallium oxide nanowires using nickel chloride ($NiCl_2$) as catalyst during a thermal CVD method. Chun *et al* [26] and Chang *et al* [27] have reported the preparation of Ga_2O_3 nanowires using Ni as a catalyst. Also, the growth of Ga_2O_3 nanowires has not been systematically studied yet.

In this paper, β-Ga_2O_3 nanowires that were successfully synthesized on silicon substrate by CVD method will be discussed. The microstructure of β-Ga_2O_3 nanomaterials was investigated by high-resolution transmission electron microscopy (HRTEM) and electron energy-loss spectroscopy (EELS). Results show that four major types of morphology were exhibited for these Ga_2O_3 nanowires during different proportions of catalysts, the particle-fused nanowires, single-crystal nanowires, nanorods and crystalline-amorphous core–shell nanowires were produced. Three β-Ga_2O_3 nanomaterials were studied in particular, single-crystal nanowires, particle-fused nanowires, crystalline-amorphous core–shell nanowires, respectively. EELS spectra analysis verified that the amorphous shell was Ga_2O_3. The growth behavior of β-Ga_2O_3 nanowires was discussed and a vapor-solid (VS) growth mechanism was proposed to explain the single crystal Ga_2O_3 nanowires.

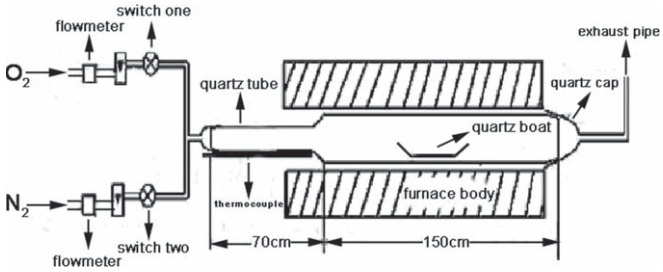

Figure 1. Schematic illustration of the CVD system.

2. Experimental

β-Ga_2O_3 nanowires were synthesized by a thermal CVD method and $NiCl_2$ catalyst were prepared by a typical chemical process. The raw materials were metal Ga powder (Aladdin, purity:99.99%), $NiCl_2{\cdot}6H_2O$ crystal (Aladdin, purity:99.9%), CaF_2 (Aladdin, purity:99.5%), O_2(purity:99.999%), N_2 (purity:99.999%) and Si (111) wafers. The samples were prepared in a high temperature diffusion furnace. A schematic of the CVD system used to grow gallium oxide nanowires is shown in figure 1.

The silicon (111) wafer substrate was cleaned in a $NiCl_2$ solution with ethanol for 1 h, dried in air, and were placed on a quartz carrier. Then, metal gallium (Ga), calcium fluoride (CaF_2, as a dispersing agent), and metal tin powder (Sn, as the doping source) was mixed according to the required proportions of the experiment [28, 29]. The flow rate of O_2 and N_2 is the same (100 sccm). Firstly, N_2 with flow rate of 100 sccm was used to drive the remaining air out and lasted for 5 min, and then the 30 min oxygen oxidation, finally ventilation the 10 min nitrogen to drive residual oxygen. The weight ratio of Ga/CaF_2/Sn in the mixture is 1:2:0.02, and the mixture of Ga/CaF_2/Sn and the Si substrate are in the same boat.

They were ground for 30 min to an agate mortar. When the furnace was heated to an equilibrium temperature of 1050 °C, flowing nitrogen was introduced into the tube for 5 min to flush the air. Next, the quartz boat with the Si (111) wafers and evaporated source powders was pushed into the constant thermal region of the furnace. Oxygen was added from the other side (time depending on the experimental conditions), then flushed with nitrogen for 10 min. Finally, the samples can be removed from the quartz boat. The volume percentage of $NiCl_2$ is 1%, 2%, 4%, respectively.

The microstructure of the samples was investigated using a JEOL 2100 F transmission electron microscopy (TEM). EELS was performed on an FEI Tecnai F20 TEM. All the EELS spectra were acquired in image mode with a collection half-angle of ~16 m rad.

3. Results and discussion

3.1. Microstructure of β-Ga_2O_3 nanomaterials

Figure 2 displays the morphologies of the synthesized β-Ga_2O_3 nanomaterials which were measured by TEM. It is clear that the β-Ga_2O_3 nanomaterials have four different micro-morphologies: particle-fused nanowires, single-crystal nanowires, nanorods, and core–shell nanowires. Figure 2(a) shows the β-Ga_2O_3 nanowires formed by the fusion of particles. The β-Ga_2O_3 nanowires are composed of many Ga_2O_3 nanoparticles with a diameter of about 180 nm and are in an irregular arrangement. Figure 2(b) shows the TEM bright field image of a single crystal Ga_2O_3 nanowires. As seen in the figure, the surface of the nanowire is smooth, varies in length from tens of nanometers to several hundred nanometers, and the diameter of the nanowires is about 30 nm. In previous reports, the length of prepared Ga_2O_3 nanowires is generally several hundred nanometers, the diameter of the Ga_2O_3 nanowires is several tens of nanometers [30]. figure 2(c) shows Ga_2O_3 nanorods. The surface of the nanorods is smooth. The length ranges from 300 nm to 1.3 μm and the diameter is about 150 nm. Figure 2(d) is a transmission electron microscopy picture of the β-Ga_2O_3 nanowires with a core–shell structure. It can be seen easily in the figure that the nanowires have a core–shell structure. The core is a monocrystalline Ga_2O_3, the shell is amorphous Ga_2O_3, the diameter of the nanowires is about 40 nm, and the thickness of the shell is about 30 nm shown by the follow-up high resolution TEM image and EELS analysis. The different microstructure of β-Ga_2O_3 nanomaterials is results from the different ratio of the catalyst. When the ratio of the catalyst is 1%, the nanowires are mainly composed of nanocrystals. When the ratio of the catalyst is 2%, the main product is single crystal nanowires which have partial core–shell nanowires. When the proportion of catalyst ratio is increased to 4%, the main products are nanorods and partial core–shell nanowires. The reasons for this phenomenon are as follows: when the proportion of catalysts is small, it is too small to play a role in guiding the growth of nanowires,

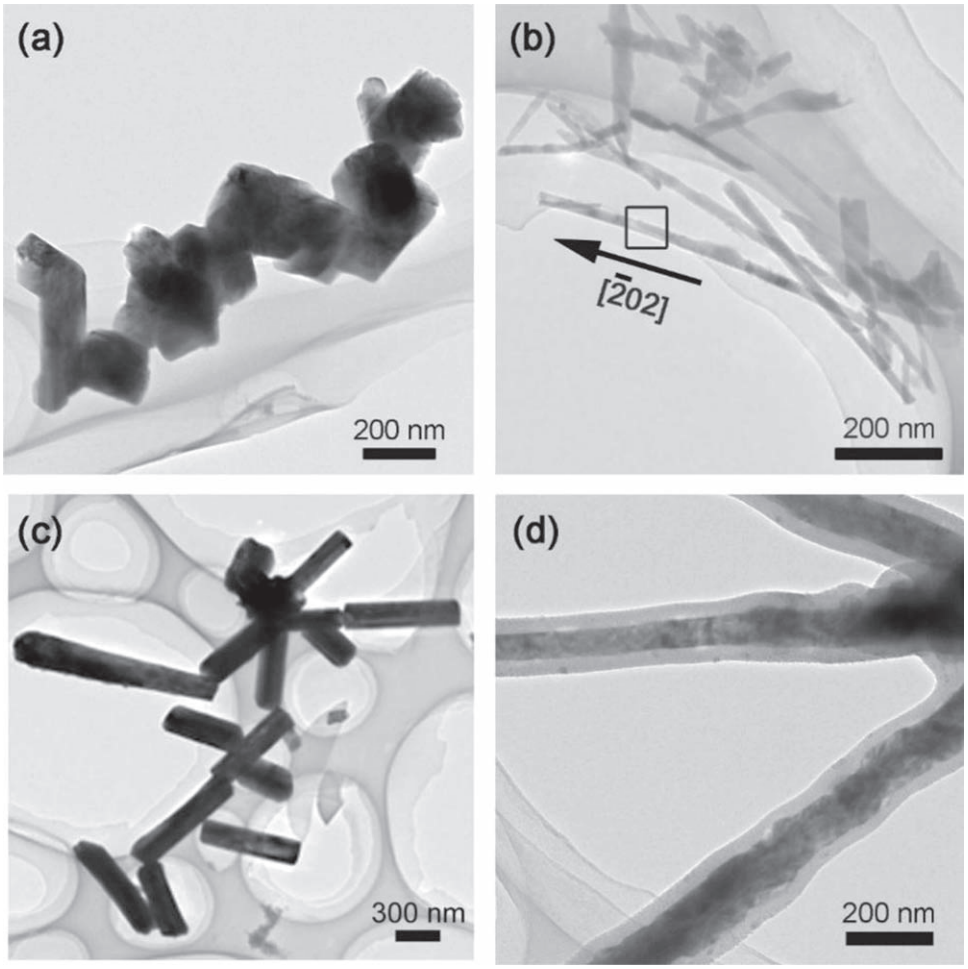

Figure 2. (a) A low-magnified TEM image of β-Ga_2O_3 nanowires, $NiCl_2$ 1%; (b) The morphology of β-Ga_2O_3 nanomaterials, $NiCl_2$ 2%. (c) The morphology of Ga_2O_3 nanorod, $NiCl_2$ 4%; (d) The morphology of β-Ga_2O_3 nanowires with a core–shell structure, $NiCl_2$ 2%.

therefore, the main product is particle-fused nanowires. When the proportion of catalyst increases, single crystal nanowires and core–shell nanowires appear. $NiCl_2$ acts as catalyst and plays an important role in the growth of the β-Ga_2O_3 nanowires, because Ni^{2+} is probably the nucleation point of the β-Ga_2O_3 embryos. The nanowires with core–shell structure were also obtained. This may be because the local distribution of the catalyst was not uniform, which resulted in the late crystallization of part Ga_2O_3, so the core–shell structure appeared.

3.2. TEM characterization and growth mechanism of β-Ga_2O_3 nanowires

Firstly, the characterization of monocrystalline β-Ga_2O_3 single crystal nanowires was studied. Figure 3 shows the scanning electron microscopy of Ga_2O_3 nanowires on the Si substrate. A large number of Ga_2O_3 nanowires were present on the Si substrate and were irregularly arranged. Figure 3(b) is a rectangular area of the enlarged picture. Careful observation reveals the surface of the nanowire is smooth and the thickness is relatively uniform. In addition, there is no orientation between the nanowires and the substrate, indicating that the nanowires are not epitaxially grown on the substrate. A more detailed crystal structure was revealed by HRTEM mode and SAED. The HRTEM images of Ga_2O_3 nanowires are displayed in figures 4(a) and (b). The clear lattice fringes confirm that the synthesized nanowires are single crystals. The closest interplanar distance is about 0.29 nm which corresponds the crystal ($\bar{2}$02) plane of β-Ga_2O_3. This indicates that the growth direction of the nanowire is [$\bar{2}$02]. Furthermore, the lattice is very perfect which indicates that the nanowire is a high-quality crystal lattice with no defects. The corresponding SAED pattern in figure 4(a) also reveals that the nanowire is monoclinic β-Ga_2O_3 and its growth direction is [$\bar{2}$02].

Figure 4(a) shows the HRTEM image of a single nanowire. Here, the nanowires are single crystal structures with a single nanowire diameter of about 40 nm and smooth. This is consistent with the results of scanning electron microscopy. The graphs in figure 4(a) are the constitutive electron diffraction patterns of nanowires according to the unit cell parameters of β-Ga_2O_3: a $=$ 4.98 Å, b $=$ 4.98 Å, c $=$ 13.43 Å, $\alpha = \beta = 90°$, and the calibration results are shown in the illustration. The diffraction spots are arranged in regular periods, and the

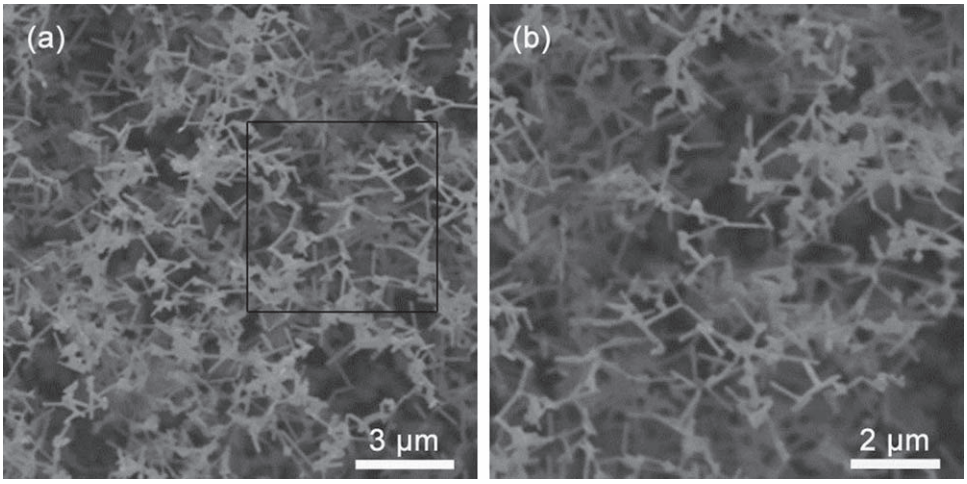

Figure 3. The morphology of β-Ga_2O_3 nanowires, β-Ga_2O_3 nanomaterias oxidized for 30 min, the ratio of $NiCl_2$ (catalyst) was 2%.

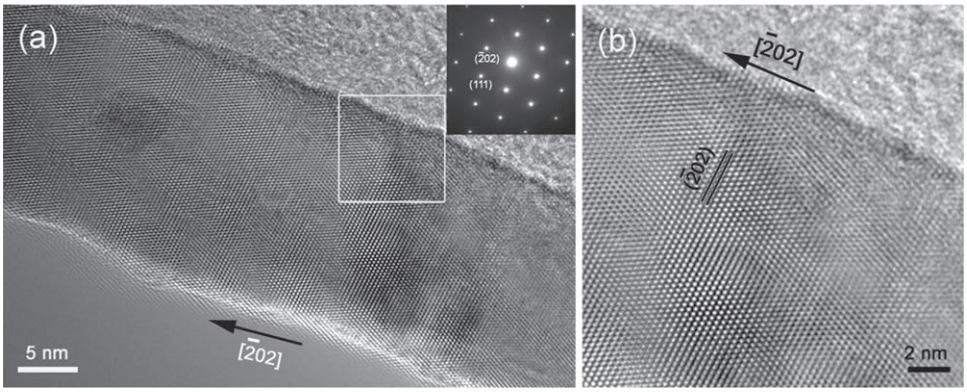

Figure 4. (a) A low-magnified TEM image of β-Ga_2O_3 nanowires. The inset shows corresponding SAED pattern recorded along the [$\bar{2}$02] zone axis; (b) The enlarged RTEM image of a white rectangular box marked in (a). The ratio of $NiCl_2$ (catalyst) was 2%, β-Ga_2O_3 nanomaterias oxidized for 30 min.

β-Ga_2O_3 is a single crystal structure. Figure 4(b) shows a high-resolution image of the rectangular area in figure 4(a). The crystal plane spacing of the resulting material is 2.91 Å, corresponding to a crystal plane ($\bar{2}$02) of β-Ga_2O_3 (d($\bar{2}$02)=2.82 Å). In the monoclinic structure, the direction perpendicular to ($\bar{2}$02) is [$\bar{2}$02]. The growth direction of this nanowire is [$\bar{2}$02], as indicated by the black arrow in the figure.

Secongly, we further studied the growth mechanism of β-Ga_2O_3 single crystal nanowires. At present, the growth mechanism of one-dimensional nanomaterials mainly includes vapor-liquid-solid (VLS) [31, 32] vapor-solid-solid (VSS) [33] and vapor-solid (VS) [34] growth mechanism. It has reported that when use the catalyst, the growth would follow the VLS and VSS mechanism [26]. The classical characteristic of the VLS and VSS mechanism is that there is droplet observed at the top of the one-dimensional nanomaterials. In this expertiment, $NiCl_2$ was used as catalyst, but no catalyst particles were found on the tip of the prepared Ga_2O_3 nanowire, so it was inferred that VLS and VSS mechanism was not suitable for our results. Unlike VLS and VSS methods, the VS method generally does not require the intervention of an external catalyst. Instead it uses the crystal itself to extend the growth rate of other crystals in different growth rates [35, 36]. Without catalyst, the growth of β-Ga_2O_3 nanowires would be categorized as VS mechanism, as suggested by other groups [37, 38]. Therefore, although we use the catalyst, the VS mechanism may be more suitable for the VLS one to demonstrate the growth of Ga_2O_3 nanomaterials.

It was inferred that Ni^{2+} did not form an alloy with Ga during the growth of nanowire. During the heating process, gallium metal forms gaseous Ga atoms, which are transported by oxygen to the substrate covered by Ni^{2+}. The free gaseous Ga and O atoms are absorbed by Ni^{2+} and then react to form nuclei. As the reaction progresses, the free Ga and O atoms continue to diffuse and grow along the preferred orientation, and finally Ga_2O_3 nanowire is obtained. Figure 5 shows the growth mechanism of Ga_2O_3 nanowires.

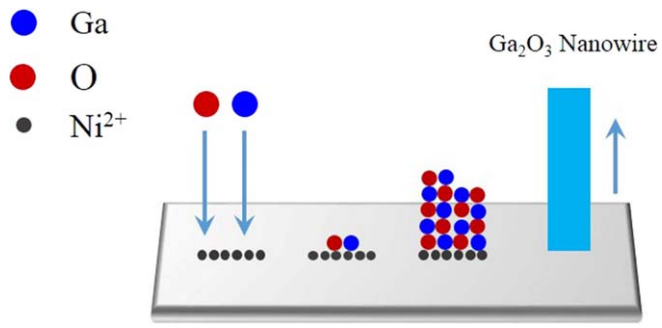

Figure 5. Growth schematic of β-Ga_2O_3 nanowire.

The chemical reaction equation for this experiment is as follows:

$$4Ga + 3O_2 \rightarrow 2Ga_2O_3$$

As shown in figure 5, there is a layer of $NiCl_2$ catalyst on the Si substrate. During the reaction, the chemical bond of Ni-Cl in $NiCl_2$ breaks to produce Ni^{2+}, which plays an important guiding role in the growth process of Ga_2O_3 nanomaterial [10, 38]. The catalytic mechanism is that Ni^{2+} can change the energy distribution of the substrate surface, that is to say, where there is a Ni^{2+} distribution, a large amount of defect energy will be generated, which leads to the growth of nanowires.

3.3. TEM study on particle fusion nanowires

When the other experimental conditions are constant and the catalyst ratio is 1%, the product is mainly pelletized nanowires. In the previous studies on Ga_2O_3 nanomaterials, few literatures have been studied the structure of particle fusion nanowires and core–shell nanowires by TEM. In this paper, the structure of particle fusion nanowires and core–shell nanowires was studied by SEM and TEM, respectively. The nanowires are not pure single crystals, but are composed of many grains, as shown in figure 6. Figure 6(a) is a scanning electron microscope (SEM) image of Ga_2O_3 nanowires on the substrate. The substrate formed a layer of dense Ga_2O_3 nanowires after the reaction. With careful observation, we can see the surface of the nanowires is not smooth. The nanowires are made of a pile of grains. In order to further observe the morphology of the Ga_2O_3 nanowires, the rectangular region in (a) was enlarged, as shown in figure 6(b). It can be seen from figure 6(b) the diameter of the nanowires is about 200 nm. Figure 6(c) shows a bright field of Ga_2O_3 nanowires using TEM, where the surface of the nanowires is rough and made up of many different grains. The diameter of the nanowires is about 180 nm. Additionally, there are some bright areas marked with the rectangular in figure 6(c) in the nanowires. In order to further study the exact structure of this bright area, HRTEM was applied. As shown in figure 6(d), the bright area marked in figure 6(c) is composed by two grains. The white dotted line in the figure 6(d) indicates the interface between the nanocrystals and the different grains. In addition, it can be observed that the lattice fringes of the lower grains are very clear and the lattice fringes of the upper grains are very blurred due to the different orientations of the grains. The plane spacing of two parallel white lines is 2.92 Å, which corresponds to the {004} plane of β-Ga_2O_3. Through the observation of TEM and SEM, two points can be obtained. First, dense Ga_2O_3 nanowires formed on the substrate, and the surface of the nanowires is rough with no fixed growth direction. Second, Ga_2O_3 nanowires are made of different grain piles, and there is no fixed orientation between the grains.

3.4. TEM study on β-Ga_2O_3 nanowires with core–shell structure

In the process of preparing β-Ga_2O_3 nanowires, we found that there was another form of β-Ga_2O_3 nanowires synthesized when the catalyst was increased to 2%, the core–shell structure of the β-Ga_2O_3 nanowires shown in figure 7. Figure 7(a) is a field TEM image of a single core–shell structure nanowires. It is clear that the nanowires have a core–shell structure, the diameter is about 60 nm, and the shell thickness is about 40 nm. Compared with monocrystalline nanowires, the core–shell nanowires have a relatively large diameter. The constitutive electron diffraction pattern, which can be seen from the diffraction point clear, is arranged neatly. Figure 7(b) shows the HRTEM image of the core–shell structure β-Ga_2O_3 nanowires. The core is single crystal, and the spacing between two parallel white lines is 5.71 Å. This corresponds to the (100) crystal plane ($d_{(100)} = 5.60$ Å) of β-Ga_2O_3. The growth direction of the core–shell nanowires is [100], as shown by the black arrow in figure 7(a). This is different from the growth direction [$\bar{2}02$] of the single crystal nanowires studied earlier. The shell is an obviously amorphous. In order to confirm the specific composition of the core–shell, an EELS analysis was produced and is shown in figure 8.

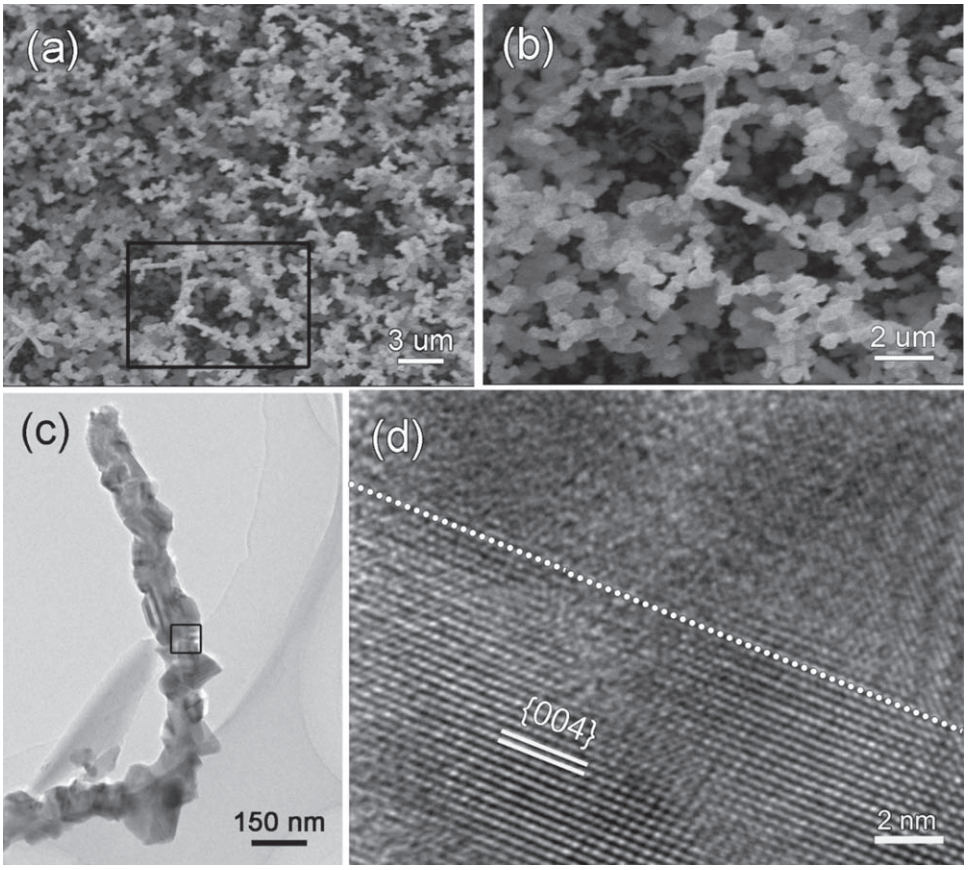

Figure 6. (a) Typical scanning electron microscope image of the Ga_2O_3 nanowire; (b) The magnified image of the rectangular area in (a); (c) Typical TEM image of the Ga_2O_3 nanowire; (d) Typical HRTEM image for the nanowire. The ratio of $NiCl_2$ (catalyst) was 1%, β-Ga_2O_3 nanomaterials oxidized for 15 min.

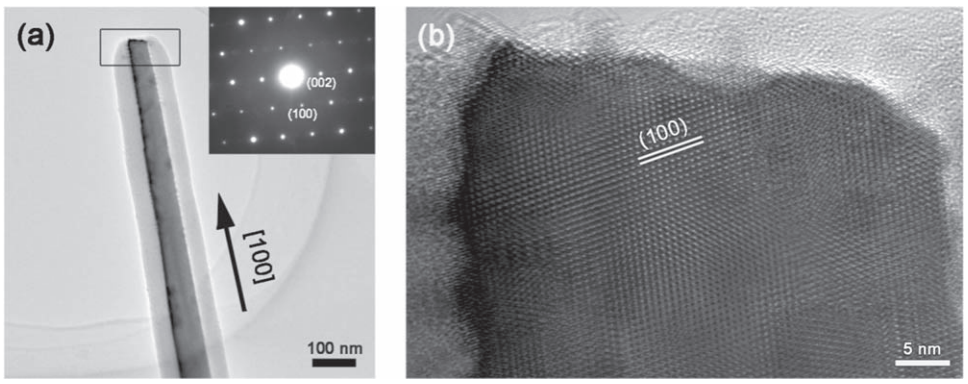

Figure 7. (a) A low-magnified TEM image of β-Ga_2O_3 nanowires, The inset shows corresponding SAED pattern recorded along the [100]; (b) The enlarged HRTEM image of a white rectangular box marked in (a). The ratio of $NiCl_2$ (catalyst) was 2%, β-Ga_2O_3 nanomaterials oxidized for 15 min.

Figure 8 shows the EELS spectrum were obtained from the amorphous shell on the surface of nanowire corresponding to figure 7(a). Figure 8(a) shows the EELS of O-*K*. The characteristic peak is about 536 eV, which corresponds to the O-*K* ionization loss peak, (b) is the EELS of Ga-$L_{2,3}$, with a peak at about 1222 eV, corresponding to Ga-$L_{2,3}$. This allows us to assume that the amorphous region has two elements, O and Ga, and the composition of the amorphous region is Ga_2O_3. Thus, the shell portion is uncrystallized Ga_2O_3.

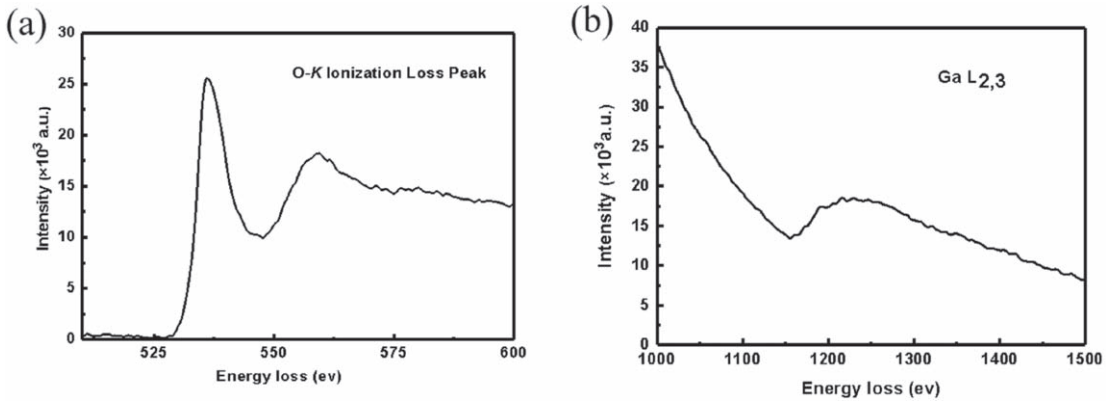

Figure 8. EELS spectra of amorphous shell of figure 7(a).

4. Conclusions

In summary, monoclinic β-Ga_2O_3 nanomaterials were successfully prepared by CVD method and were investigated by TEM. Four morphologies of β-Ga_2O_3 nanowires were obtained, grains stacked nanowires, single crystal nanowires and nanorods, core–shell structure nanowire, respectively. The results show that if the ratio of catalysts is different, morphology of β-Ga_2O_3 nanowires is different. When the ratio of catalyst is 1%, mostly stacked nanowires are obtained. When the proportion of catalyst is increased to 2%, single crystal nanowires are produced. When the catalyst ratio increased to 4%, nanorods are most common. The preferential growth orientation of the single crystal nanowires is [$\bar{2}$02] and the growth mechanism of single crystal β-Ga_2O_3 was clarified by vapor-solid growth mechanism. The existence of Ni^{2+} plays a very important role in the growth of Ga_2O_3 nanowires. It prompted Ga_2O_3 nucleation and encouraged the nanowire growth. Besides, the compositions of core–shell structure nanowire was studied, and the components of core and shell were all Ga_2O_3 which was confirmed by EELS.

Acknowledgments

The authors would like to thank the financial support from the Program of Science and Technology for Higher Education in Shandong Province (Grant no.: J12LA17), the Scientific Research Starting Foundation for Introduced Talents at Qingdao University (Grant no.: 06300701) and the natural science foundation of Shandong province (Grant no.:ZR2019PEE022). One author (B Liu) would also like to thank the financial support from National Natural Science Funds of China (Grant No. 21701095) and the financial support from the Program of Science and Technology for Higher Education in Shandong Province(Grant no.: J17KA010).

ORCID iDs

Lei Shang https://orcid.org/0000-0002-0036-204X

References

[1] Yakobson B I and Smalley R E 1997 *Am. Sci.* **85** 324 https://www.jstor.org/stable/27856810?seq=1#page_scan_tab_contents
[2] Hu J T, Odom T W and Lieber C M 1999 *Acc. Chem. Res.* **32** 435
[3] Dong L F, Jiao J, Tuggle D W, Petty J, Elliff S A and Coulter M 2003 *Appl. Phys. Lett.* **82** 1096
[4] Pan Z W, Dai Z R and Wang Z L 2001 *Science* **291** 1947
[5] Law M, Kind H, Kim F, Messer B and Yang P 2002 *Angew. Chem.* **41** 2405
[6] Alivisatos A P 1996 *Science* **271** 933
[7] Wong E W, Sheehan P E and Lieber C M 1997 *Science* **277** 1971
[8] Ginly D S and Bright C 2000 *Mater. Res. Soc. Bull.* **25** 15
[9] Yamazoe N 1991 *Sens. Actuator s* B **5** 7
[10] Shi F and Feng X W 2012 *J. Nanosci. Nanotechnol.* **12** 8481
[11] Wei J, Zang Z J, Xue C S and Shi F 2015 *J. Mater. Sci., Mater. Electron.* **26** 1368
[12] Wei J and Shi F 2016 *J. Mater. Sci., Mater. Electron.* **27** 942
[13] Chun H J, Choi Y S, Bae S Y, Seo H W, Hong S J, Park J and Yang H 2003 *J. Phys. Chem.* B **107** 9042
[14] Zhang H Z, Kong Y C, Wang Y Z, Du X, Bai Z G, Wang J J, Yu D P, Ding Y, Hang Q L and Feng S Q 1999 *Solid State Commun.* **109** 677
[15] Liang C H, Meng G W, Wang G Z, Wang Y W and Zhang L D 2001 *Appl. Phys. Lett.* **78** 3202

[16] Kim B C, Sun K T, Park K S, Im K J, Noh T, Sung M Y and Kim S 2002 *Appl. Phys. Lett.* **80** 479
[17] Terasakoa T, Kawasakib Y and Yagi M 2016 *Thin Solid Films* **620** 23
[18] Han N *et al* 2014 *Nanoscale Res. Lett.* **9** 347
[19] Park G S, Choi W-B, Kim J-M, Choi Y C, Lee Y H and Lim C-B 2000 *J. Cryst. Growth* **220** 494
[20] Yamahara H, Seki M and Tabata H 2012 *J. Cryst. Process Technol.* **2** 125
[21] Zhu F, Yang Z X, Zhou W M and Zhang Y F 2006 *Appl. Surf. Sci.* **252** 7930
[22] Gao Y H, Bando Y, Sato T, Zhang Y F and Cao X Q 2002 *Appl. Phys. Lett.* **81** 2267
[23] Gundiah G, Govindaraj A and Rao C N R 2002 *Chem. Phys. Lett.* **351** 189
[24] Cui L F and Ruffo R 2009 *Nano Lett.* **9** 491–5
[25] Jiang G J *et al* 2000 *J. Mater. Sci.* **35** 63
[26] Chun H J *et al* 2003 *J. Phys. Chem.* B **107** 9042
[27] Chang K W and Wu J J 2003 *Appl. Phys.* A **629** 76
[28] Shi F and Xue C 2011 *J. Mater. Sci., Mater. Electron.* **22** 1835
[29] Shi F, Gu Y F and Li C X 2014 *Adv. Mater. Res.* **873** 200
[30] Kumar S, Srinivas Goud B and Singh R 2013 *J. Nano- Electron. Phys.* **5** 02003 https://jnep.sumdu.edu.ua/en/component/search/index.php?option=com_content&task=full_article&id=925
[31] Terasako T, Yagi M, Ishizaki M, Senda Y, Matsuura H and Shirakata S 2007 *Surf. Coat. Technol.* **22-23** 8924
[32] Han N *et al* 2012 *Cryst. Growth Des.* **9** 6243
[33] Yang Z X *et al* 2013 *Nanoscale.* **9** 9671
[34] Wagner R S and Ellis W C 1964 *Appl. Phys. Lett.* **89** 4
[35] Lee J S *et al* 2002 *J. Cryst. Growth* **244** 287
[36] Zhao Y F *et al* 2014 *J. Mater. Sci., Mater. Electron.* **25** 181
[37] Zhang H Z *et al* 1999 *Solid State Commun.* **109** 677
[38] Kim B C *et al* 2002 *Appl. Phys. Lett.* **80** 479